



## Hourly Variations and Potential Sources of Airborne Trace Elements in PM<sub>10</sub> in Four Representative Regions of Southeastern China

Huajun Ye<sup>1,2\*</sup>, Kai Yang<sup>3</sup>, Xuejiao Jiang<sup>2</sup>, Lili Niu<sup>4</sup>, Daozhu Hua<sup>2</sup>, Dan Li<sup>2</sup>, Shuihe Shi<sup>5</sup>

<sup>1</sup> State Key Laboratory of Modern Optical Instrumentation, Zhejiang University, Hangzhou 310027, China

<sup>2</sup> Focused Photonics (Hangzhou), Inc., Hangzhou 310052, China

<sup>3</sup> China National Environmental Monitoring Center, Beijing 100000, China

<sup>4</sup> College of Environmental & Resource Sciences of Zhejiang University, Hangzhou 310058, China

<sup>5</sup> Environmental Monitoring Station of Dongming County, Heze 274500, China

### ABSTRACT

Aerosol pollution episodes have frequently occurred in China in recent years, and the airborne trace elements in particulate matter have been a cause for concern worldwide because of their impacts on human health. However, there is limited information on the hourly variations of airborne trace elements. This paper describes a detailed investigation conducted in March 2013 on the hourly variations and potential sources of airborne trace elements. Trace elements in particles with aerodynamic diameters less than 10 μm (PM<sub>10</sub>) were monitored on-line in four representative regions with similar latitudes in southeastern China. Our results showed that the number of species of elements in PM<sub>10</sub> detected at urban sites and an industrial park was greater than that at a rural site, due to the influences of human activities. The hourly variation patterns of trace elements indicated that their concentrations were stable during the day at the rural site, whereas a visible “double peak” of Pb and Cu was observed in the tourist city and a “single morning peak” of Pb and As was seen in the industrial city. These variations indicated the abundant traffic in the tourist city, and strong industrial emissions in the industrial city. However, the single morning peak and the slight double peak patterns of the trace elements were both found at the industrial park, indicating a combined source of industry and traffic. The results from the source identification also indicated that the sources of airborne elements were mainly industrial emissions at industrial sites, whereas the elements in the tourist city might primarily result from traffic. The correlations between PM<sub>10</sub> concentrations and trace element concentrations were also studied. The results revealed that PM<sub>10</sub> correlated better with elements originating from natural sources (e.g., K, Ca, Fe) than with those from anthropogenic sources (e.g., Pb, Zn, Cu). Our results provide a scientific basis for pollution control strategies at these sites.

**Keywords:** Trace elements; PM<sub>10</sub>; Hourly variation; Potential sources.

### INTRODUCTION

Atmospheric pollution has become one of the top environmental issues in China due to the rapid industrialization and motorization in the past few decades. Aerosols in the atmosphere can adversely affect human health via inhalation, especially in the urban environment (Poschl, 2005). As important components of aerosols, trace elements have been a cause for concern worldwide due to their impacts on the human health (Chapman *et al.*, 1997; Ghio *et al.*, 1999).

Trace elements in atmospheric particulate matter are

derived from both natural and anthropogenic sources. Natural emissions can result from forest fires and the oceans as well as a variety of processes acting on crustal minerals, such as volcanism, erosion, and surface winds (Allen *et al.*, 2001). Crustal elements, such as Na, Mg, Al, K, Ca, Sc, Ti, V, Mn, Fe, As, and Ba, substantially contribute to the total natural emissions of trace metals to the atmosphere (Cong *et al.*, 2011). Furthermore, anthropogenic origins, including industrial processes (such as mining, metal smelting, oil combustion, and waste incineration), transportation and agricultural activities (Gibb *et al.*, 2003; Pacyna *et al.*, 2009), are the main sources of toxic metalliferous particles. Elements emitted to the atmosphere by industrial metallurgical processes include As, Cd, Cu, Ni, and Zn, whereas the combustion of fossil fuels is the principal anthropogenic source of Be, Co, Hg, Mo, Ni, Sb, Se, Sn, V, As, Cr, Cu, Mn, and Zn (Pacyna, 1998). Traffic pollution involves a wide range of trace element emissions, including Pb, Fe, Cu, Zn,

\* Corresponding author.

Tel.: 86-0751-8501-2188; Fax: 86-0571-8501-2006  
E-mail address: huajun\_ye@fpi-inc.com

Cr, Sn, Sb, Ni, and Cd. Additionally, tire rubber abrasion is a major source of Zn (Pacyna, 1998; Birmili *et al.*, 2006; Amato *et al.*, 2009; Bukowiecki *et al.*, 2010). Elements mainly original from anthropogenic origins were called “anthropogenic elements”, such as Pb, Zn, Cd, As, Cr and Ni, etc. (Cong *et al.*, 2011).

Many studies have focused on the pollution problems from airborne trace elements with aerodynamic diameters less than 10  $\mu\text{m}$  ( $\text{PM}_{10}$ ) (Helble *et al.*, 1996; Vasconcelos and Tavares, 1998; Pio *et al.*, 1998; Yatin *et al.*, 2000; Shotyk *et al.*, 2001; Gao *et al.*, 2002). In these studies, however, particle samples were collected by a manual sampler and underwent chemical analysis in the laboratory. These processes were not only complex and time-consuming but also had low sampling frequencies and required a delay in the data analysis. Moreover, few of these studies involved the hourly variations of airborne trace elements and the potential major sources of these elements in various representative regions, both of which are valuable for generating pollution control strategies.

In this study, the concentrations and hourly variations of airborne trace elements in  $\text{PM}_{10}$  were monitored on-line in four different representative regions (a rural area, an industrial park far from urban areas, a famous tourist city, and a typical industrial city) in southeastern China using an Atmospheric Heavy Metals Continuous Monitoring System. In addition, the enrichment factors and the varimax rotated principal component analysis were employed to identify the potential

sources of the airborne trace elements. Furthermore, the correlations between  $\text{PM}_{10}$  concentrations and airborne trace element concentrations at an urban site were calculated. This study provides fingerprint characteristics of airborne trace elements in four regions in China, which will be valuable for optimizing air pollution control strategies.

## METHODS

### Sampling Sites

The sampling and detection of  $\text{PM}_{10}$ -bound elements were conducted at four representative sites (A, B, C, and D) in southeastern China (Fig. 1). Site A, B, and C were located in rural area, industrial park and urban area, respectively, in Zhejiang province. For a more comprehensive study of airborne trace elements in  $\text{PM}_{10}$  in different representative regions, site D located in a famous industrial city in Hubei province was chosen for comparison with other sites.

Site A is located at a rural site (Taizhou city, Zhejiang province, China), without any pollution. Site B is located in an industrial park (Huzhou city, Zhejiang province, China), far from any urban area. The main industrial activities in this area involve lead-acid battery production and industrial metallurgical processes. An emissions stack is located approximately 400 m to the southwest of site B. Site C is a traffic-impacted urban site located along a roadside in Hangzhou, which is one of the most famous tourist city in China. The urban nucleus of Hangzhou has more than 6

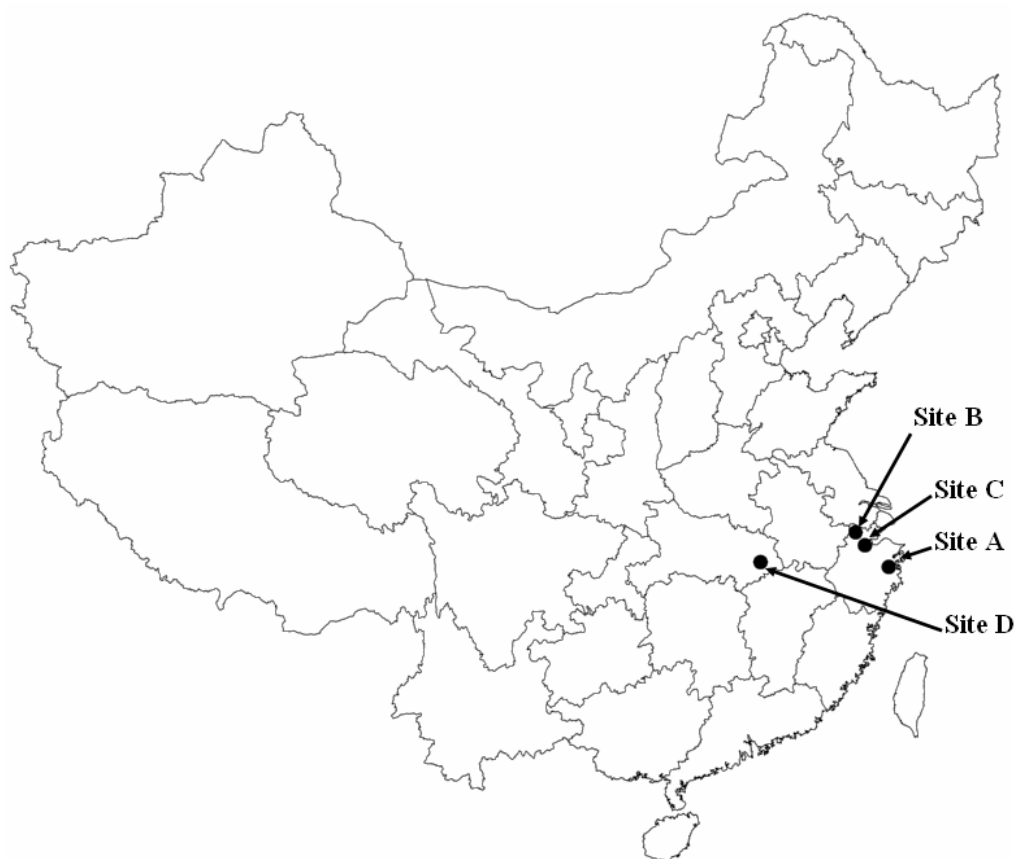


**Fig. 1.** Monitoring site locations.

million inhabitants, and thus heavy traffic. It is worth noting that there are construction sites in the vicinity of site C. Site D is an urban site located in Huangshi, an industrial city in Hubei province. Including the surrounding areas, there are about 2.6 million inhabitants. The city has flourishing mining and metallurgical industries with iron ore in the northwest, copper mines and nonferrous metal plants in the southwest, and a cement plant in the southeast. All experiments were conducted on the rooftops of tall buildings at the four sites (approximately 20 m above ground level).

### Sampling and Analysis

The determinations of airborne trace elements were performed every 2 hours from March 1 to March 31, 2013 at the four sites using Atmospheric Heavy Metals Monitoring Systems (AMMS, Focused Photonics (Hangzhou), Inc., China), which performed rapid, non-destructive analysis of the airborne trace elements. A 2- $\mu\text{m}$  Teflon filtering membrane tape was used to filter and deposit the aerosols. The flow rate of AMMS is 16.67 L/min. The content of the airborne elements was then detected by the XRF analyzer in the AMMS. The volume of gas that passed through the filtering membrane was recorded by a mass flow meter. The concentrations of the trace elements can be calculated based on the mass of trace elements deposited on the filtering membrane and the total sampling gas volume (Ye *et al.*, 2012a, b).

In this study, a total of 21 elements (Fe, K, Ca, Mn, Ba, Ti, Sc, Cr, As, Pb, V, Cd, Zn, Cu, Se, Hg, Ni, Sb, Sn, Mo, and Co) were simultaneously measured by the AMMS. Elemental concentrations were quantified using external XRF calibration standards (XRF calibration standards, Micromatter, Vancouver, Canada). One or two checks were completed every month after the initial calibration. The method detection limits (MDLs), defined as three times the standard deviations of replicate blank measurements, of K, Ca, Sc, Ti, Ba, V, Cr, Mn, Fe, Co, Ni, Cu, Zn, Hg, As, Se, Pb, Mo, Cd, Sn, and Sb were 4.2, 3.2, 0.82, 0.98, 1.81, 0.31, 0.52, 0.63, 1.28, 0.5, 0.65, 6.94, 6.31, 0.62, 0.34, 0.5, 0.71, 0.8, 5.5, 9.05, and 12.18  $\text{ng}/\text{m}^3$ , respectively. The

precisions (relative standard deviation values of replicate standard measurements) for all the element concentrations were less than 2%. To study the accuracy of the AMMS with trace elements, we measured the trace element concentrations in  $\text{PM}_{10}$  simultaneously using the AMMS and a standard method in our earlier study (Ye *et al.*, 2012b), in which a standard  $\text{PM}_{10}$  sampler (Laoying 2030, Qingdao Laoshan Applied Technology Research Institute, Qingdao, China) was used to collect  $\text{PM}_{10}$ , and the filter sample was analyzed by ICP-MS in the lab. The flow rate of the  $\text{PM}_{10}$  sampler was set at 100 L/min with sample collection time 100 min. The particles were filtered through a 0.45  $\mu\text{m}$  cellulose acetate filter with 80 mm diameter, which had relative low element content. The filters were digested in the lab and the element content in the filters was determined by ICP-MS (X series II, Thermo Fisher Inc., USA). The AMMS samplings with a flow rate of 16.67 L/min were conducted simultaneously with the standard  $\text{PM}_{10}$  sampler. The particles were deposited on the Teflon filtering membrane tape and then the content of the airborne elements was detected by the XRF analyzer in the AMMS. For most elements, the relative error between AMMS results and the standard method results was less than 15%, such as Pb, Fe, K and Ca, etc. Fig. 2 shows the results for the determinations of Pb and Fe by the AMMS and the standard method. It was found that the correlation between the AMMS and the standard method was better than 0.98 (Ye *et al.*, 2012b).

The determinations of airborne trace elements were performed every 2 hours (100min for sampling, 20min for analyzing and filter tape moving) during March 2013 using the AMMSs at all the four sites, and there were 355, 356, 347 and 342 valid data sets in site A, B, C and D, respectively. The sampling time, the sampling volume, the average temperature and the average atmospheric pressure were simultaneously recorded. The flow and concentration checks were conducted before and after this campaign to ensure that the data is valid.

The  $\text{PM}_{10}$  concentration was also measured every two hours, synchronized with trace element monitoring (10 days from March 7 to March 17, 2013), at site D using a

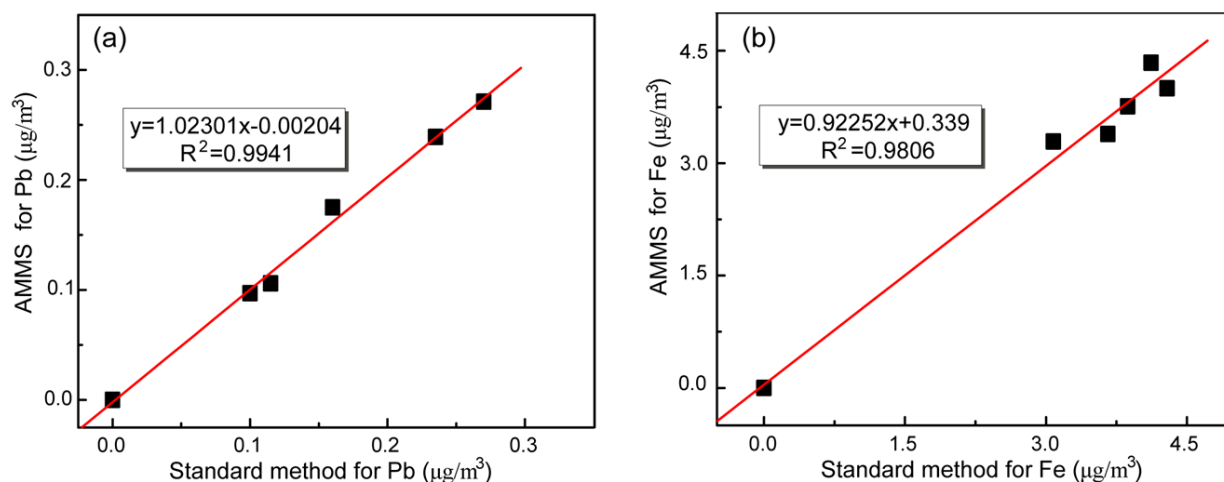


**Fig. 2.** Comparisons between the AMMS and the standard method for the determinations of Pb (a) and Fe (b).

Continuous Monitoring System (BPM-200, Focused Photonics (Hangzhou), Inc., China) based on a  $\beta$ -ray absorption method. The detection limit of the BPM-200 is  $5 \mu\text{g}/\text{m}^3$ . There were 120 valid data sets and each set contained the sampling time, the sampling volume, the average temperature, the average atmospheric pressure and the concentrations ( $\mu\text{g}/\text{m}^3$ ) of  $\text{PM}_{10}$ .

## RESULTS AND DISCUSSION

### *Elemental Composition and Concentration in $\text{PM}_{10}$*

The monthly mean and geometric standard deviations of elemental concentrations in  $\text{PM}_{10}$  at the four sites (Table 1) were used for further discussion. Mean concentrations lower than the XRF method detection limits were excluded from the following analysis. These elements included 1) Hg, Cd, Cu, Sb, Sn, Co, and Mo at site A; 2) Hg at site B; and 3) Hg and Co at site C.

As shown in Table 1, the total element concentrations at the urban sites (sites C and D) were much higher than those at the rural site (site A) and the industrial park (site B). The number of element species detected in the urban areas (sites C and D) and the industrial park (site B) was greater than in the rural area (site A), indicating the obvious influence of human activities on the atmospheric environment.

For straightforward comparison, the elements of the four sites in Table 1 were grouped into four categories (Table 2). According to the concentrations and categories described above, Fe, K, and Ca were the main elements in  $\text{PM}_{10}$ , which agrees with previous research by Cong *et al.* (2011). The proportions of Fe, K, and Ca were the highest in the

rural area (site A) and the lowest at the industrial park (site B). These three elements accounted for approximately 84.8% and 73.3% of all metals studied in  $\text{PM}_{10}$  at sites A and B, respectively. The proportions of anthropogenic elements in  $\text{PM}_{10}$  were relatively lower than the crustal elements except for Pb and Zn, which had concentrations comparable to some crustal elements such as Ti, Ba, and Mn. As shown in Table 2, Zn was grouped in Category 1 in the urban areas (sites C and D) but in Category 2 in the rural area (site A) and the industrial park (site B). However, Pb was grouped in Category 2 at the industrial sites (site B and D) but in Category 3 in the rural area (site A) and the tourist city (site C). It is worth noting that Cu was grouped in Category 2 only in the industrial city (site D), and its concentration at site D was much higher than at the other three sites. The Cu concentration might be influenced by the copper mine in the southeast of the industrial city.

As the primary anthropogenic elements in the atmosphere, Pb and Zn often showed higher concentrations than other anthropogenic elements. Therefore, detailed investigations were conducted of these two elements at the four sites. The concentrations of Pb were  $354.7$ ,  $171.5$ , and  $92.1 \text{ ng}/\text{m}^3$  at sites D, B, and C, respectively. These values are much larger than that at site A ( $43.2 \text{ ng}/\text{m}^3$ ). The high content of Pb at site D may be primarily due to the mixed industrial emissions of the industrial city. However, the high content of Pb at site B should be mainly from the local lead-acid battery production in the industrial park. Finally, abundant traffic may be the mainly origin of the high content of Pb at site C. In contrast, the Zn concentrations decreased in the following order: site C ( $877.9 \text{ ng}/\text{m}^3$ ) > site D ( $507.6 \text{ ng}/\text{m}^3$ ) >

**Table 1.** Concentrations of airborne trace elements in  $\text{PM}_{10}$  during March, 2013 ( $\text{ng}/\text{m}^3$ ).

Elements	Site A		Site B		Site C		Site D	
	Mean	S.D.	Mean	S.D.	Mean	S.D.	Mean	S.D.
Pb	43.2	30.9	171.5	256.3	92.1	82.9	354.7	968.0
Se	1.0	1.5	5.5	2.8	1.5	2.4	12.6	14.8
Hg	—	—	—	—	—	—	0.7	0.8
Cr	20.8	13.5	91.1	18.4	10.5	14.5	33.0	67.3
Cd	—	—	45.3	38.1	29.5	50.5	20.1	47.3
Zn	125.6	125.9	131.3	102.2	877.9	452.9	507.6	632.9
Cu	—	—	70.9	59.3	34.2	80.4	289.9	379.2
Ni	8.7	11.5	7.6	5.3	12.6	18.6	20.9	20.5
Fe	1316.2	1234.8	1206.3	1115.4	2285.2	1820.7	2628.6	2592.7
Mn	165.4	101.3	236.2	49.8	55.3	48.1	83.7	78.3
Ti	123.6	129.7	102.0	107.9	136.9	107.6	110.9	105.5
Sb	—	—	19.6	38.4	24.6	54.4	18.5	43.3
Sn	—	—	46.5	55.4	24.2	50.8	18.0	42.2
V	4.4	3.2	20.2	4.6	0.4	1.6	2.2	4.3
Ba	104.3	69.7	124.2	64.0	128.6	107.1	140.8	170.6
As	3.9	5.8	2.6	4.9	15.9	14.2	144.7	372.4
Ca	1298.7	1131.8	1121.4	815.3	3451.1	2809.6	3168.3	3335.6
K	804.0	590.6	762.0	394.6	967.1	440.0	1516.8	1788.7
Co	—	—	5.0	3.3	—	—	3.5	6.5
Mo	—	—	35.2	35.8	5.1	14.2	4.4	16.1
Sc	13.7	15.2	12.3	7.2	89.9	76.0	38.7	41.4
Total	4033.5	2845.8	4216.7	2335.6	8242.6	5452.1	9118.7	7670.3

“—” means under detection limit.

**Table 2.** Categories of airborne trace elements in PM<sub>10</sub>.

	Category 1 > 500 ng/m <sup>3</sup>	Category 2 (100–300) ng/m <sup>3</sup>	Category 3 (10–100) ng/m <sup>3</sup>	Category 4 < 10 ng/m <sup>3</sup>
Site A	Fe, K, and Ca	Mn, Ti, Ba, and Zn	Pb, Cr, and Sc	Se, Ni, V, and As
Site B	Fe, K, and Ca	Mn, Ti, Ba, Zn, and Pb	Cd, Cr, Cu, Sb, Sn, V, Mo, and Sc	Se, Ni, Co, and As
Site C	Fe, K, Ca, and Zn	Ti and Ba	Pb, Cd, Cr, Ni, Cu, Sb, Sn, As, Mn, and Sc	Se, Mo, and V
Site D	Fe, K, Ca, and Zn	Cu, Ti, Ba, and Pb	Cd, Cr, Ni, Sb, Sn, As, Mn, and Sc	Se, Mo, Co, and V

site B (125.9 ng/m<sup>3</sup>)  $\approx$  site A (125.6 ng/m<sup>3</sup>). The high Zn concentration at site C indicated the presence of traffic pollution, although it might have been affected by both industrial and traffic emissions at site D.

Site B had the highest concentrations of Cr, Sn, V, and Mo of the four sites, and the cumulative proportion of the four elements was 4.6% of the total elements, whereas only 0.63%, 0.5% and 0.6% at site A, C and D, respectively. It has been reported that elements such as Cr, Sn, V, and Mo most likely originate from the combustion of fossil fuels (Pacyna, 1998). This conclusion is supported by the higher proportions of Cr, Sn, V, and Mo found at the industrial park site in our study. Antimony, which has been reported to be a traffic-related constituent from brake linings (Lee *et al.*, 1994; Weckwerth, 2001), had the highest concentration in the tourist city (site C). Additionally, as a typical crustal element, Sc had the highest concentration at site C, which could be a result of the construction activity nearby. The concentrations of Cu, Ni, and As were the highest at the industrial city site (site D), with a total proportion of 5.0%. However, the proportion of these elements was only 1.9% at site B, which is also affected by industrial emissions. This result could be explained by the more complex influences of the industries at site D compared with site B.

To further compare the element concentrations in particle matter, data from other typical regions was listed in Table 3, such as Beijing, the capital of China (Duan *et al.*, 2014), Shijiazhuang, a typical industrial city in northern China (Wang, 2004), Wuhan, a big city near Huangshi (site D) in Hubei province (Lv *et al.*, 2006), Shanghai, a big economic city near Hangzhou (site C) (Chen *et al.*, 2008), Foshan, a typical industrial city in southern China (Tan *et al.*, 2014), Agra, India in southern Asia (Kulshrestha *et al.*, 2009) and Budapest, Hungary in European (Maenhaut *et al.*, 2005). As shown in Table 3, the concentrations of trace elements in site A were much lower than other regions in China, and generally comparable with some European urban sites such as Budapest, Hungary (Maenhaut *et al.*, 2005). Site B was located in an industrial park far from any urban area, and the concentrations of most crustal elements such as Fe, Ca, K, Ba, Ti and Sc at site B were comparable with site A, whereas the concentrations of anthropogenic elements such as Pb, Cd, Cr, Cu etc. at site B were much higher than those at site A. Almost all the elements at site C and D had lower concentrations than Shijiazhuang (Wang, 2004) and Foshan (Tan *et al.*, 2014), the typical industrial cities in northern and southern China, respectively, except Cu and As at site D. In addition, the concentrations of most elements at site C were lower than those in Beijing (Duan *et al.*, 2014), Wuhan (Lv *et al.*, 2006), Shanghai (Chen *et*

*al.*, 2008), and the averaged concentrations in China (Duan and Tan, 2013), except Cd and Zn, which were original from the abundant traffic of the tourist city. However, the concentrations of most elements at site D were comparable with those in Beijing (Duan *et al.*, 2014), Wuhan (Lv *et al.*, 2006), Shanghai (Chen *et al.*, 2008), and the averaged concentrations in China (Duan and Tan, 2013), except for Cu and As, which had high concentrations due to the local industry at site D. Compared with some regions abroad, the element concentrations in the tourist city (site C) and the industrial city (site D) were much higher than those in some European urban areas (Hueglin *et al.*, 2005; Maenhaut *et al.*, 2005; Limbeck *et al.*, 2009) but much lower than that in some cities in southern Asia (Kulshrestha *et al.*, 2009; von Schneidemesser *et al.*, 2010).

#### Hourly Variations

The variation of meteorological conditions and source emission strength over time may affect the characteristics of particulate matter. Therefore, hourly variations of airborne trace elements in PM<sub>10</sub> at the four sites are described in this paper. The mean concentrations of the typical elements at 1:00, 3:00, 5:00, 7:00, 9:00, 11:00, 13:00, 15:00, 17:00, 19:00, 21:00 and 23:00 of the four sites during March, 2013 were shown in Fig. 3. The mean concentration of a typical element at one time was calculated using concentrations at the same time in different days, for example, the mean concentration of Pb at 7:00 at site C was calculated using the concentrations at 7:00 every day in March 2013 at site C. Each mean concentration was calculated using about 30 values. In addition, the range and hourly variation pattern of trace element concentrations at the four sites were also shown in Fig. 3. There were striking differences in the hourly variation patterns of the average concentrations of the trace metals at the four sites. In addition, these hourly concentrations showed a wide range of values due to the different meteorological conditions and source emission strength in the same time of different days.

As shown in Figs. 3(a) and 3(b), the concentrations of Pb and Ba were stable during the day at site A. However, there were two slight peaks in Pb concentration during rush hour in the morning and evening and a third peak at approximately 01:00 (LST) at site B (Fig. 3(c)). Additionally, a small single concentration peak of Cd was found in the morning at site B (Fig. 3(d)). At site C, double peak patterns of Pb and Cu were found during rush hour (Figs. 3(e) and 3(f)), which is similar to the Cu and Sb concentration patterns in Barcelona, Spain found by Moreno *et al.* (2011). During the morning, there was a single peak of Pb and a single, prolonged peak of As at site D (Figs. 3(g) and 3(h)).

**Table 3.** Concentration levels of airborne trace elements in different typical regions (ng/m<sup>3</sup>).

	This study			Averaged levels in China <sup>a</sup>	Beijing <sup>b</sup>	Shijia-Zhuang <sup>c</sup>	Wuhan <sup>d</sup>	Shanghai <sup>e</sup>	Foshan <sup>f</sup>	Agra, India <sup>g</sup>	Budapest, Hungary <sup>h</sup>
	site A	site B	site C								
Pb	43.2	171.5	92.1	354.7	281.6	462.0	415.6	108.5	675.7	1100.0	24.0
Se	1.0	5.5	1.5	12.6	—	—	—	—	—	—	—
Hg	—	—	—	0.7	—	—	—	—	—	—	—
Cr	20.8	91.1	10.5	33.0	41.6	321.0	14.0	27.3	—	300.0	8.9
Cd	—	45.3	29.5	20.1	5.8	—	9.0	2.9	42.6	—	—
Zn	125.6	131.3	877.9	507.6	501.9	1656.0	604.4	418.5	2214.0	500.0	84.0
Cu	—	70.9	34.2	289.9	72.2	162.0	36.9	35.5	283.8	40.0	61.0
Ni	8.7	7.6	12.6	20.9	22.7	73.0	6.5	10.0	—	200.0	3.2
Fe	1316.2	1206.3	2285.2	2628.6	—	—	—	—	—	2900.0	1930.0
Mn	165.4	236.2	55.3	83.7	163.7	577.0	155.6	60.3	170.9	900.0	30.0
Ti	123.6	102.0	136.9	110.9	—	—	—	—	—	—	73.0
Sb	—	19.6	24.6	18.5	—	—	—	—	—	—	—
Sn	—	46.5	24.2	18.0	—	—	—	—	—	—	—
V	4.4	20.2	0.4	2.2	10.7	78.8	11.5	10.3	40.0	—	—
Ba	104.3	124.2	128.6	140.8	—	—	—	—	—	—	—
As	3.9	2.6	15.9	144.7	47.1	—	46.9	30.8	76.6	—	52.0
Ca	1298.7	1121.4	3451.1	3168.3	—	—	—	—	—	—	1.4
K	804.0	762.0	967.1	1516.8	—	—	—	—	—	—	—
Co	—	5.0	—	3.5	—	—	—	—	—	—	0.5
Mo	—	35.2	5.1	4.4	—	—	—	—	—	—	—
Sc	13.7	12.3	89.9	38.7	—	—	—	—	—	—	—

“—” means under detection limit or not determined.

a (Duan and Tan, 2013).

b PM<sub>10</sub>, Beijing, December 2006 (Duan *et al.*, 2014).

c PM<sub>10</sub>, Shijiazhuang, January 2001 (Wang, 2004).

d PM<sub>10</sub>, Wuhan, September 2003 - September 2004 (Lv *et al.*, 2006).

e PM<sub>2.5</sub>, Shanghai, March 2004 - March 2005 (Chen *et al.*, 2008).

f PM<sub>2.5</sub>, Foshan, December 2008 (Tan *et al.*, 2014).

g PM<sub>10</sub>, Agra, India, May 2006 - March 2008 (Kulshrestha *et al.*, 2009).

h PM<sub>10</sub>, Budapest, Hungary, spring 2002 (Maenhaut *et al.*, 2005).

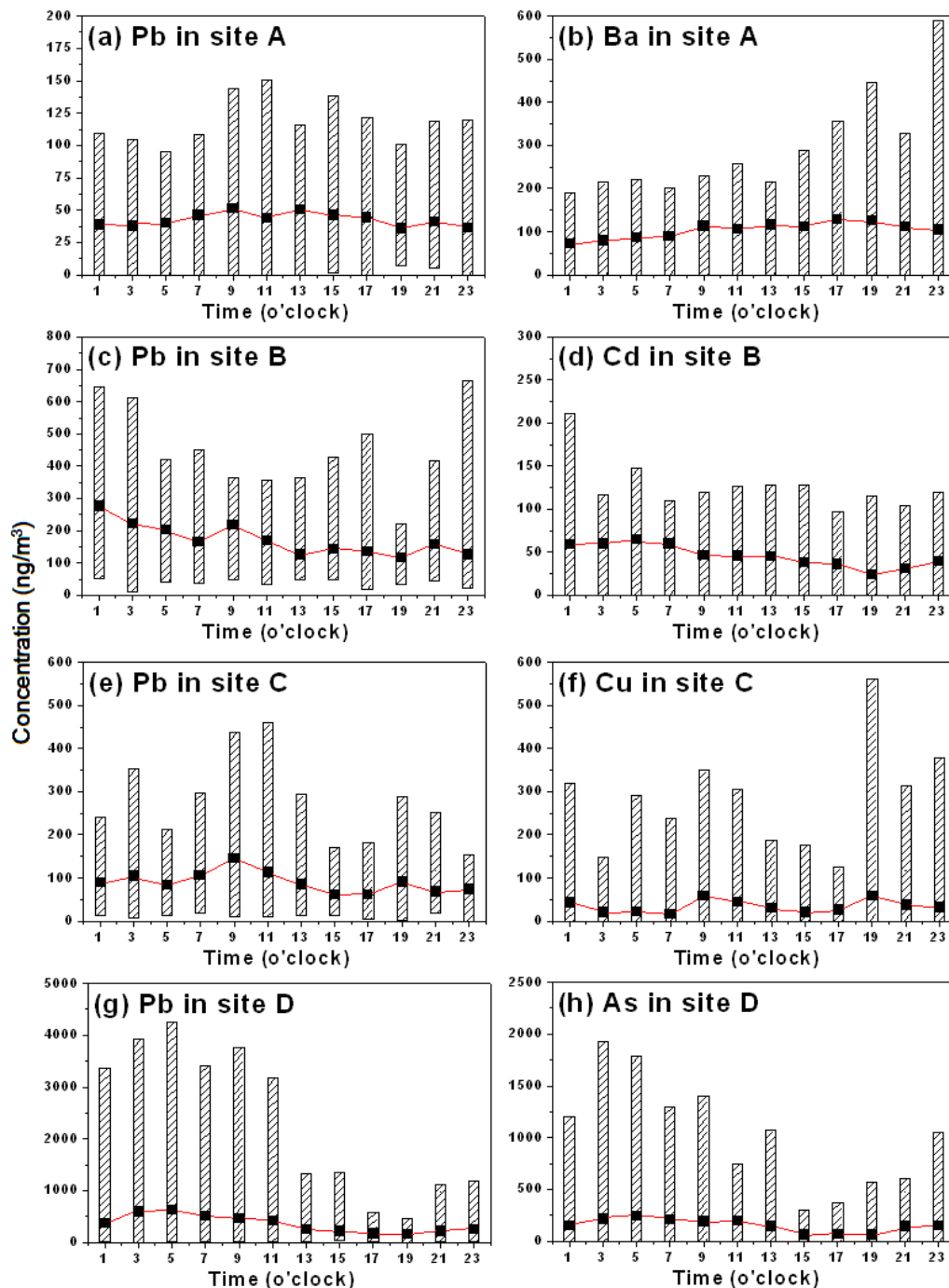


**Fig. 3.** Average (black squares), range (shaded columns) and hourly variation patterns (red lines) of trace element concentrations (ng/m<sup>3</sup>) obtained at the four sites.

Site A was located in a rural area, and fugitive dust may have been the primary source of trace elements at this site. Therefore, the variation patterns of the element concentrations were relatively stable during the day at site A (Figs. 3(a) and 3(b)). Pb was one of the main pollutants at site B due to its location at an industrial park. The two Pb peaks at rush hour in the morning and evening should be attributed to the traffic in this industrial park. The other peak in Pb concentration at approximately 01:00 (LST) at site B should be due to the industrial emissions of this industrial park. In

addition, there was a slight peak in the Cd concentration in the morning at site B, indicating that industrial emissions were the main source of Cd at the industrial park. Sites C and D were both located in urban areas, and the sources of trace elements should be very complex. However, obvious double peak patterns of Pb and Cu at site C (Figs. 3(e) and 3(f)) and single morning peak patterns of Pb and As at site D (Figs. 3(g) and 3(h)) were found. These peaks suggest that traffic and industrial emissions were the dominant sources of trace elements at sites C and D, respectively.

### Sources of Trace Elements

To identify the potential sources of the trace elements, the enrichment factor (EF) for each element was calculated. The EF concept is based on the fact that metals originating from relatively well-defined sources (such as Fe or Mn constituting the primary component of the earth's crust) can be distinguished from other metals derived from different source processes (Taylor, 1964). Therefore, the EF values of the trace elements in the four regions were calculated to identify their potential sources. The EF of a given element in an aerosol sample is defined as

$$EF = \frac{[E]_{air}/[R]_{air}}{[E]_{crust}/[R]_{crust}} \quad (1)$$

where E denotes an element of interest and R is a reference element.  $[E]_{air}$  and  $[R]_{air}$  are the concentrations of elements E and R in  $PM_{10}$ , respectively. Similarly,  $[E]_{crust}$  and  $[R]_{crust}$  are the concentrations of elements E and R, respectively, in the earth's crust. In this paper, Fe was used as a reference element, and the composition of the earth's crust was taken from Taylor (1964).

Most of the elements were mainly influenced by crustal dusts ( $EF < 10$ ), anthropogenic sources ( $EF > 100$ ), and mixed sources ( $10 < EF < 100$ ) (Song *et al.*, 2012). As shown in Table 4, the EF values of most elements were less than 10 in the rural area (site A). In the industrial park (site B), the EF values of Pb, Se, Cd, Sb, Sn, and Mo were 640.4, 5147.6, 10571.6, 4579, 1084, and 1094, respectively. These values demonstrated that anthropogenic emissions, such as lead-acid battery production (Pb and Cd) and combustion emissions (Se, Sb, Sn, and Mo) (Pacyna, 1998),

were the dominant contributors. There were many elements with EF values much greater than 100 in both the tourist city (Pb, Se, Cd, Zn, Sb, Sn, As, and Sc) and the industrial city (Pb, Se, Hg, Cd, Zn, Cu, Sb, Sn, and As), indicating that the sources in these two urban regions were more complex than those in the rural area and the industrial park. Therefore, a varimax rotated principal component analysis (PCA) was performed using SPSS 16.0 software to identify the potential sources of the trace elements at sites C (347 data sets) and D (342 data sets), and the results were shown in Table 5.

As shown in Table 5, our analysis extracted 5 contributing factors at site C. Elements from the fugitive dust, such as Fe, Ba, Ca, Ti, Sc, Mn, K, and Cr, were highly loaded in the first factor, which accounted for 42.4% of the total variance. Fugitive dust in the tourist city (site C) might be attributed to resuspension processes, such as traffic movement. The ubiquitous construction activities near site C during the campaign were also potential contributors. This result is in agreement with previous research by Cong *et al.* (2011), who found that fugitive dust of natural origin was the main factor in elements in  $PM_{10}$ . Furthermore, the second, third, and fourth factors extracted at site C were all associated with traffic elements. These factors are in agreement with Song *et al.* (2012), who found that traffic elements, such as Pb, Zn, and Cu, were secondary factors influencing the total element sources in Beijing. Importantly, China phased out leaded gasoline in 1998, and the lead content in fuel is now limited to less than 0.013 g/L (Wu *et al.*, 2011). Vehicle emissions should no longer be an overwhelming source of Pb. However, Pb is widely used in a number of car components, including lead wheel weights, solder in electronics, and lead-acid batteries. The deterioration of such components may generate particles containing Pb.

**Table 4.** Enrichment factors (EF) of trace elements in  $PM_{10}$  at the four sites.

Element	Enrichment factors			
	Site A	Site B	Site C	Site D
Pb	147.7	640.4	181.5	607.7
Se	855.5	5147.6	730.0	5405.7
Hg	—	—	—	197.7
Cr	8.9	42.5	2.6	7.1
Cd	—	10571.6	3630.7	2157.7
Zn	76.7	87.6	309.0	155.3
Cu	—	60.2	15.3	112.9
Ni	5.0	4.7	4.1	6.0
Fe	1.0	1.0	1.0	1.0
Mn	7.4	11.6	1.4	1.9
Ti	0.93	0.83	0.59	0.42
Sb	—	4579.0	3036.2	1982.5
Sn	—	1084.7	297.6	193.0
V	1.4	7.0	0.06	0.35
Ba	10.5	13.6	7.5	7.1
As	93.4	68.7	217.4	1721.7
Ca	1.3	1.3	2.0	1.6
K	1.6	1.7	1.1	1.6
Co	—	9.3	—	3.0
Mo	—	1094.4	84.0	62.9
Sc	26.6	26.0	100.7	37.7



**Table 5.** Varimax rotated factor loading matrix for elements in PM<sub>10</sub> at sites C and D.

	Site C						Site D					
	Factor 1	Factor 2	Factor 3	Factor 4	Factor 5	Factor 6	Factor 1	Factor 2	Factor 3	Factor 4	Factor 5	Factor 6
Fe	<b>0.978</b>	As <b>0.894</b>	Sb <b>0.938</b>	Cu <b>0.909</b>	V <b>0.981</b>	Cr <b>0.789</b>	0.881	As <b>0.911</b>	Sn <b>0.846</b>	Cu <b>0.859</b>	K <b>0.956</b>	Cr <b>0.789</b>
Ba	<b>0.971</b>	Pb <b>0.817</b>	Cd <b>0.934</b>	Ni <b>0.891</b>		V <b>0.638</b>	0.88	Pb <b>0.908</b>	Mo <b>0.824</b>	Ni <b>0.803</b>	Ba <b>0.842</b>	V <b>0.638</b>
Ti	<b>0.964</b>	Zn <b>0.718</b>	Sn <b>0.913</b>				0.869	Hg <b>0.765</b>	Sb <b>0.813</b>	Co <b>0.709</b>		
Ca	<b>0.947</b>	Se <b>0.63</b>					0.798	Cd <b>0.716</b>	Cd 0.443			
Sc	<b>0.94</b>	Cr 0.426					0.712	Se <b>0.697</b>				
Mn	<b>0.913</b>						0.427	Zn <b>0.686</b>				
K	<b>0.91</b>						0.423					
Cr	<b>0.712</b>											
Variance (%)	42.398	16.874	10.556	8.594	5.654		33.5	16.2	12.6	8.8	7.5	6.1
Cumulative (%)	42.398	59.272	69.829	78.423	84.077		33.5	49.7	62.2	71	78.5	84.5
Source type	Crust-1	Tra.-1	Tra.-2	Tra.-2	Crust-2		Crust-1	Ind.-1	Mixed	Ind.-2	Crust-2	Crust-3

Tra., Ind., and Com. are abbreviations for traffic, industry, and combustion, respectively.

Moreover, there was almost no coal burning in the vicinity of site C in Hangzhou which was also regarded a major source of Pb (Duan *et al.*, 2012), and the obvious double peak hourly variation pattern of Pb (Fig. 3(e)) during rush hour at site C also suggested that vehicle emissions could still be one of the major sources of Pb (Harrison *et al.*, 1996; Simcik *et al.*, 1999; Allen *et al.*, 2001; Song *et al.*, 2012). V, an element that may come from both crustal and anthropogenic sources (Samara *et al.*, 1994; Harrison *et al.*, 1996; Miranda *et al.*, 1996; Swietlicki *et al.*, 1996; Pacyna, 1998; Moreno *et al.*, 2011; Tan *et al.*, 2014), was highly correlated with the fifth factor at site C. Since the EF value of V at site C was much less than 10 (Table 4), V was from crustal source.

The first factor extracted at site D, which explained 33.5% of the total variance, was strongly correlated with natural elements (Fe, Ca, Sc, Ti, and Mn) (Table 5). Similarly, the crustal elements K and Ba were highly correlated with the fifth factor at site D from natural sources. Unlike site C, the Pb, As, and Ni at site D had hourly variations significantly associated with industrial emissions. Therefore, industrial emissions were the dominant sources of the second and fourth factors at site D. However, the third factor, which had high loadings of Sn, Mo, Sb, and Cd at site D, was likely correlated with mixed sources from industry (Cd), traffic (Sb), and combustion (Mo and Sn). Finally, V and Cr with EF values both less than 10 were highly loaded in the sixth factor extracted at site D, suggested that the sixth factor was mainly correlated with nature sources.

#### Relationship between PM<sub>10</sub> and Trace Elements

Elements from anthropogenic sources have very low concentrations and are significantly influenced by source emission strength. However, elements from natural sources are primarily influenced by meteorological conditions, similar to PM<sub>10</sub> (Cong *et al.*, 2011). Therefore, the relationship between PM<sub>10</sub> and trace elements was studied further using 120 sets of data for every two hours from March 7 to March 17, 2013 at site D. The highest correlation was found between K and PM<sub>10</sub> ( $R = 0.925$ ,  $P < 0.0001$ ) (Fig. 4(a)), whereas the lowest correlation was found between Pb and PM<sub>10</sub> ( $R = 0.153$ ,  $P < 0.1$ ) (Fig. 4(b)). The correlation coefficient between PM<sub>10</sub> and Fe was 0.5 ( $P < 0.0001$ ) while 0.59 ( $P < 0.0001$ ) between PM<sub>10</sub> and Ca. However, the correlation between PM<sub>10</sub> and Cu was 0.25 ( $P < 0.01$ ) and 0.19 ( $P < 0.1$ ) between PM<sub>10</sub> and Zn. It is suggested that the distribution patterns of crustal elements were similar to PM<sub>10</sub>, whereas those of anthropogenic elements were different. Our results are consistent with Cong *et al.* (2011), who has also found that crustal elements had similar seasonal variations with PM<sub>10</sub>. These results also suggest that natural elements preferentially concentrate in PM<sub>10</sub> more than elements influenced by anthropogenic sources and the proportion of crustal elements in PM<sub>10</sub> was more stable than the proportion of anthropogenic elements in PM<sub>10</sub>.

#### CONCLUSIONS

In this study, trace elements in PM<sub>10</sub> were determined at

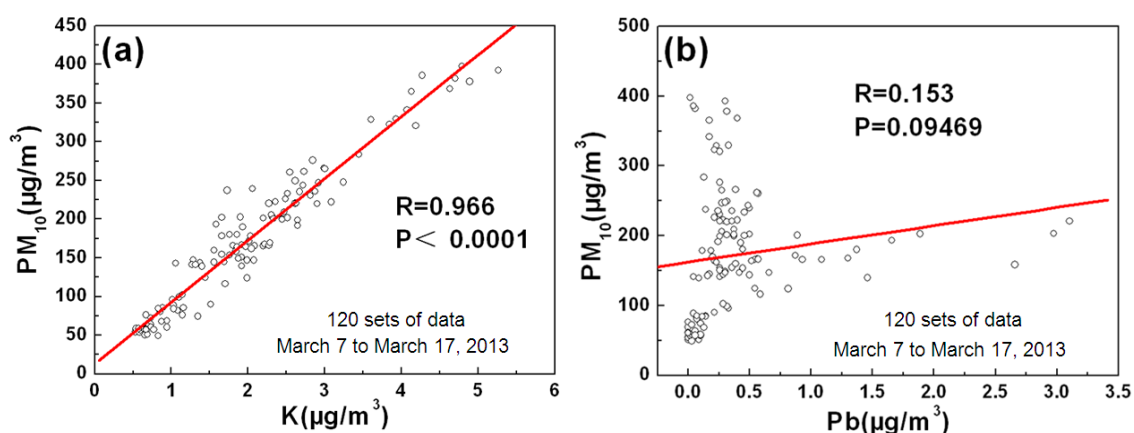


**Fig. 4.** Correlations between  $PM_{10}$  and trace elements at site D. (a)  $PM_{10}$  vs. K; (b)  $PM_{10}$  vs. Pb.

four sites in southeastern China (a rural area, an industrial park, a tourist city, and an industrial city) during March 2013. The total element concentrations at the urban sites were much higher than those at the rural site or the industrial park. In addition, more species of elements were detected in  $PM_{10}$  at the urban sites and the industrial park, indicating the influence of human activities. Different hourly variations of airborne trace elements were found in the four regions due to different sources. Elements in the rural area usually had stable concentrations without any obvious peaks. “Double peak” and “single morning peak” patterns in element concentrations were both found at site B, indicating the combined industrial and traffic sources in the industrial park. An obvious double peak pattern associated with the abundant traffic in the tourist city was found for Pb and Cu. The single morning peak of Pb and As at site D indicated the strong industrial emissions in the industrial city. Additionally, the potential sources of airborne elements were identified by EFs and PCA. The major sources of elements in the industrial park (site B) were lead-acid battery production (Pb and Cd) and combustion emissions (Se, Sb, Sn, and Mo). The element sources in  $PM_{10}$  were more complicated at sites C and D, where the abundant traffic and industrial emissions were the dominant sources, respectively. The relationships between  $PM_{10}$  and trace elements were analyzed at site D. The results demonstrated that concentrations of elements originating from natural sources (e.g., K, Ca, Fe) had a stronger correlation with  $PM_{10}$  concentrations than those from anthropogenic sources (e.g., Pb, Zn, Cu). All the results obtained in this study could be useful for optimizing pollution control strategies in China.

#### ACKNOWLEDGMENTS

This work was supported with funding from two Major National Scientific Instrument Projects (No. 2013YQ060569 and No. 2012YQ060147).

#### REFERENCES

Allen, A.G., Nemitz, E., Shi, J.P., Harrison, R.M. and

- Greenwood, J.C. (2001). Size Distributions of Trace Metals in Atmospheric Aerosols in the United Kingdom. *Atmos. Environ.* 35: 4581–4591.
- Amato, F., Pandolfi, M., Viana, M., Querol, X., Alastuey, A. and Moreno, T. (2009). Spatial and Chemical Patterns of  $PM_{10}$  in Road Dust Deposited in Urban Environment. *Atmos. Environ.* 43: 1650–1659.
- Birmili, W., Allen, A., Bary, F. and Harrison, R. (2006). Trace Metal Concentrations and Water Solubility in Size-fractionated Atmospheric Particles and Influence of Road Traffic. *Environ. Sci. Technol.* 14: 1144–1153.
- Bukowiecki, N., Lienemann, P., Hill, M., Furger, M., Richard, A., Amato, F., Prevot, A., Baltensperger, U., Buchmann, B. and Gehrig, R. (2010).  $PM_{10}$  Emission Factors for Non-exhaust Particles Generated by Road Traffic in an Urban Street Canyon and Along a Freeway in Switzerland. *Atmos. Environ.* 44: 2330–2340.
- Chapman, R.S., Watkinson, W.P., Dreher, K.L. and Costa, D.L. (1997). Ambient Particulate Matter and Respiratory and Cardiovascular Illness in Adults: Particle-borne Transition Metals and the Heart-lung Axis. *Environ. Toxicol. Pharmacol.* 4: 331–338.
- Chen, J.M., Tan, M.G., Li, Y.L., Zheng, J., Zhang, Y.M., Shan, Z., Zhang, G.L. and Li, Y. (2008). Characteristics of Trace Elements and Lead Isotope ratios in  $PM_{2.5}$  from Four Sites in Shanghai. *J. Hazard. Mater.* 156: 36–43.
- Cong, Z.Y., Kang, S. C., Luo, C.L., Li, Q., Huang, J., Gao, S.P. and Li, X.D. (2011). Trace Elements and Lead Isotopic Composition of  $PM_{10}$  in Lhasa, Tibet. *Atmos. Environ.* 45: 6210–6215.
- Duan, J., Tan, J., Wang, S., Hao, J. and Chai, F. (2012). Size Distributions and Sources of Elements in Particulate Matter at Curbside, Urban and Rural Sites in Beijing. *J. Environ. Sci.* 24: 87–94.
- Duan, J. and Tan, J. (2013). Atmospheric Heavy Metals and Arsenic in China: Situation, Sources and Control Policies. *Atmos. Environ.* 74: 93–101.
- Duan, J., Tan, J., Hao, J. and Chai, F. (2014). Size Distribution, Characteristics and Sources of Heavy Metals in Haze Episode in Beijing. *J. Environ. Sci.* 26: 189–196.
- Gao, Y., Nelson, E.D., Field, M.P., Ding, Q., Lia, H., Sherrella, R.M., Gigliottib, C.L., Ryb, D.A., Glenn,

- T.R. and Eisenreich, S.J. (2002). Characterization of Atmospheric Trace Elements on PM<sub>2.5</sub> Particulate Matter over the New York-New Jersey Harbor Estuary. *Atmos. Environ.* 36: 1077–1086.
- Ghio, A.J., Stonehuerner, J., Dailey, L.A. and Carter, J.D. (1999). Metals Associated With both the Water-soluble and Insoluble Fractions of an Ambient Air Pollution Particle Catalyze an Oxidative Stress. *Inhalation Toxicol.* 11: 37–49.
- Gibb, W., Quick, W. and Salisbury, M. (2003). Monitoring and Control of Trace Elements, In *Technology Status Review*, Report No. COAL R249 DTI/Pub URN 03/1582.
- Harrison, R.M., Smith, D.J.T. and Luhana, L. (1996). Source Apportionment of Polycyclic Aromatic Hydrocarbons Collected from an Urban Location in Birmingham, UK. *Environ. Sci. Technol.* 30: 825–832.
- Helble, J.J., Mojtahedi, W., Lyyr nen, J., Jokiniemi, J. and Kauppinen, E. (1996). Trace Element Partitioning during Coal Gasification. *Fuel* 75: 931–939.
- Hueglin, C., Gehrig, R., Baltensperger, U., Gysel, M., Monn, C. and Vonmont, H. (2005). Chemical Characterisation of PM<sub>2.5</sub>, PM<sub>10</sub> and Coarse Particles at Urban, Nearcity and Rural Sites in Switzerland. *Atmos. Environ.* 39: 637–651.
- Kulshrestha, A., Satsangi, P.G., Masih, J. and Taneja, A. (2009). Metal Concentration of PM<sub>2.5</sub> and PM<sub>10</sub> Particles and Seasonal Variations in Urban and Rural Environment of Agra, India. *Sci. Total Environ.* 407: 6196–6204.
- Lee, D.S., Garland, J.A. and Fox, A.A. (1994). Atmospheric Concentrations of Trace Elements in Urban Areas of the United Kingdom. *Atmos. Environ.* 28: 2691–2713.
- Limbeck, A., Handler, M., Puls, C., Zbiral, J., Bauer, H. and Puxbaum, H. (2009). Impact of Mineral Components and Selected Trace Metals on Ambient PM<sub>10</sub> Concentrations. *Atmos. Environ.* 43: 530–538.
- Lv, W., Wang, Y.X., Querol, X., Zhuang, X.G., Alastuey, A., Lopez, A. and Viana, M. (2006). Geochemical and Statistical Analysis of Trace Metals in Atmospheric Particulates in Wuhan, Central China. *Environ. Geol.* 51: 121–132.
- Maenhaut, W., Raes, N., Chi, X.G., Cafmeyer, J., Wang, W. and Salma, I. (2005). Chemical Composition and Mass Closure for Fine and Coarse Aerosols at a Kerbside in Budapest, Hungary, in Spring 2002. *X-Ray Spectrom.* 34: 290–296.
- Miranda, J., Andrade, E., Lopez-Suarez, A., Ledesma, R., Cahill, T.A. and Wakabayashi, P.H. (1996). A Receptor Model for Atmospheric Aerosols from a Southwestern Site in Mexico City. *Atmos. Environ.* 30: 3471–3479.
- Moreno, T., Querol, X., Alastuey, A., Reche, C., Cusack, M., Amato, F., Pandolfi, M., Pey, J., Richard, A., Pr v t, A.S.H., Furger, M. and Gibbons, W. (2011). Variations in Time and Space of Trace Metal Aerosol Concentrations in Urban Areas and Their Surroundings. *Atmos. Chem. Phys.* 11: 9415–9430.
- Pacyna, J.M. (1986). In *Toxic Metals in the Atmosphere*, Nriagu, J.O. and Davidson, C.I. (Eds.), Wiley, New York.
- Pacyna, J.M. (1998). Source Inventories for Atmospheric Trace Metals, In *Atmospheric Particles*, IUPAC Series on Analytical and Physical Chemistry of Environmental Systems, Harrison, R.M. and Grieken, R.E. (Eds.), Wiley, Chichester, UK, 5: 385–423.
- Pacyna, J.M., Pacyna, E.G. and Aas, W. (2009). Changes of Emissions and Atmospheric Deposition of Mercury, Lead, and Cadmium. *Atmos. Environ.* 43: 117–127.
- Pio, C.A., Ramos, M.M. and Duarte, A.C. (1998). Atmospheric Aerosol and Soiling of External Surfaces in an Urban Environment. *Atmos. Environ.* 32: 1979–1989.
- Poschl, U. (2005). In *Atmospheric Aerosols: Composition, Transformation, Climate and Health Effects*. Angewandte Chemie International Edition 44, p. 7520–7541.
- Samara, C., Kouimtzi, Th. and Katsoulos, G. (1994). Characterization of Airborne Particulate Matter in Thessaloniki, Greece. Part II: A Multivariate Modelling Approach for the Source Apportionment of Heavy Metal Concentrations within Total Suspended Particles. *Toxicol. Environ. Chem.* 41: 221–232.
- Shotyk, W., Weiss, D., Kramers, J.D., Freir, R., Chenurkin, A.K., Gloor, M. and Reese, S. (2001). Geochemistry of the Peat Bog at Etang de la Gru re, Jura Mountains, Switzerland, and its Record of Atmospheric Pb and Lithogenic Trace Metals (Sc, Ti, Y, Zr, and REE) since 12,370 <sup>14</sup>C yr BP. *Geochim. Cosmochim. Acta* 65: 2337–2360.
- Simcik, M.F., Eisenreich, S.J. and Liroy, P.J. (1999). Source Apportionment and Source/Sink Relationships of PAHs in the Coastal Atmosphere of Chicago and Lake Michigan. *Atmos. Environ.* 33: 5071–5079.
- Song, S.J., Wu, Y., Jiang, J.K., Yang, L., Cheng, Y. and Hao, J.M. (2012). Chemical Characteristics of Size-resolved PM<sub>2.5</sub> at a Roadside Environment in Beijing, China. *Environ. Pollut.* 161: 215–221.
- Swietlicki, E., Puri, S., Hansson, H.C. and Edner, H. (1996). Urban Air Pollution Source Apportionment Using a Combination of Aerosol and Gas Monitoring Techniques. *Atmos. Environ.* 30: 2795–2809.
- Tan, J., Duan, J., Ma, Y., Yang, F., Cheng, Y., He, K., Yu, Y. and Wang, J. (2014). Source of Atmospheric Heavy Metals in Winter in Foshan, China. *Sci. Total Environ.* 493: 262–270.
- Taylor, S.R. (1964). Abundance of Chemical Elements in the Continental Crust: A New Table. *Geochim. Cosmochim. Acta.* 28: 1273–1285.
- Vasconcelos, M.T.S.D. and Tavares, H.M.F. (1998). Atmospheric Metal Pollution (Cr, Cu, Fe, Mn, Ni, Pb and Zn) in Oporto City Derived from Results for Low-volume Aerosol Samplers and for the Moss Sphagnum Auriculatum Bioindicator. *Sci. Total Environ.* 212: 11–20.
- von Schneidmesser, E., Stone, E.A., Quraishi, T.A., Shafer, M.M. and Schauer, J.J. (2010). Toxic Metals in the Atmosphere in Lahore, Pakistan. *Sci. Total Environ.* 408: 1640–1648.
- Wang, J. (2004). Study on Source Apportionment of Airborne Particulate Using Chemical Mass Balance (CMB) in Shijiazhuang, Nankai University.
- Weckwerth, G. (2001). Verification of Traffic Emitted Aerosol Components in the Ambient Air of Cologne (Germany). *Atmos. Environ.* 35: 5525–5536.
- Wu, Y., Wang, R.J., Zhou, Y., Lin, B.H., Fu, L.X., He,

- K.B. and Hao, J.M. (2011). On-road Vehicle Emission Control in Beijing: Past, Present, and Future. *Environ. Sci. Technol.* 45: 147–153.
- Yatin, M., Tuncel, S., Aras, N.K., Olmez, I., Aygun, S. and Tuncel, G. (2000). Atmospheric Trace Elements in Ankara, Turkey: 1. Factors Affecting Chemical Composition of Fine Particles. *Atmos. Environ.* 34: 1305–1318.
- Ye, H.J., Guo, S.L., Jiang, X.J., Xia, A.L. and Wang, J. (2012a). Development of an Atmospheric Heavy Metal Analyzer Based on X-ray Fluorescence Spectroscopy. *Chin. J. Sci. Instrum.* 5: 1161–1166.
- Ye, H.J., Liao, X.F., Guo, S.L., Jiang, X.J., Yao, L. and Chen, X.S. (2012b). Development and Application of Continuous Atmospheric Heavy Metals Monitoring System Based on X-ray Fluorescence. *Adv. Mater. Res.* 518–523: 1510–1515.

*Received for review, July 1, 2014*  
*Accepted, August 29, 2014*